# Structural Characterization of *n*-Butyl-isocyanide Complexes of Cytochromes P450nor and P450cam†

Dong-Sun Lee, Sam-Yong Park, Kazuhide Yamane,‡ Eiji Obayashi, Hiroshi Hori,§ and Yoshitsugu Shiro*

*RIKEN Harima Institute/SPring-8, 1-1-1 Kouto, Mikazuki-cho, Sayo, Hyogo 679-5148, Japan, Himeji Institute of Technology, 3-2-1 Kouto, Kamigori-cho, Ako, Hyogo 678-1297, Japan, and Osaka University, Machikaneyama, Toyonaka, Osaka 560-8531, Japan*

*Received September 22, 2000; Revised Manuscript Received January 2, 2001*

ABSTRACT: Alkyl-isocyanides are able to bind to both ferric and ferrous iron of the heme in cytochrome P450, and the resulting complexes exhibit characteristic optical absorption spectra. While the ferric complex gives a single Soret band at 430 nm, the ferrous complex shows double Soret bands at 430 and 450 nm. The ratio of intensities of the double Soret bands in the ferrous isocyanide complex of P450 varies, as a function of pH, ionic strength, and the origin of the enzyme. To understand the structural origin of these characteristic spectral features, we examined the crystallographic and spectrophotometric properties of the isocyanide complexes of *Pseudomonas putida* cytochrome P450cam and *Fusarium oxysporum* cytochorme P450nor, since ferrous isocyanide complex of P450cam gives a single Soret band at 453 nm, while that of P450nor gives one at 427 nm. Corresponding to the optical spectra, we observed C−N stretching of a ferrous iron-bound isocyanide at 2145 and 2116 $cm^{-1}$ for P450nor and P450cam, respectively. The crystal structures of the ferric and ferrous *n*-butyl isocyanide complexes of P450cam and P450nor were determined. The coordination structure of the fifth Cys thiolate was indistinguishable for the two P450s, but the coordination geometry of the isocyanide was different for the case of P450cam [d(Fe−C) = 1.86 Å, ∠Fe−C−N = 159°] versus P450nor [d(Fe−C) = 1.85 Å, ∠Fe−C−N = 175°]. Another difference in the structures was the chemical environment of the heme pocket. In the case of P450cam, the iron-bound isocyanide is surrounded by some hydrophobic side chains, while, for P450nor, it is surrounded by polar groups including several water molecules. On the basis of these observations, we proposed that the steric factors and/or the polarity of the environment surrounding the iron-bound isocyanide significantly effect on the resonance structure of the heme(Fe)-isocyanide moiety and that differences in these two factors are responsible for the spectral characteristics for P450s.

Cytochrome P450 (P450)[1] is a generic name given for *b*-type cytochromes, which exhibit Soret absorption around 450 nm on complex formation with CO (*1*−*3*). P450 catalyzes monooxygenation, as well as a variety of other biological reactions, which includes the oxidation of sulfur, epoxidation, cleavage of carbon−carbon bonds, alkyl group migration, and aromatization. Through these catalytic reactions, the P450 enzymes are involved in numerous physiologically important processes including steroid metabolism, drug deactivation, procarcinogen activation, fatty acid metabolism, xenobiotic detoxification, and the catabolism of exogenous compounds as a source of energy. Therefore, the P450 enzymes are widely distributed in nearly all eukaryotes, prokaryotes, and even in hyperthermophilic archaea. Over 1000 P450 genes have been identified to date, and comprise the P450 gene superfamily (*4*).

P450 was first found in microsomes in 1962 as a pigment, which exhibited a characteristic optical absorption spectrum (*1*, *2*). At that time, the absorption spectrum of its ethyl isocyanide complex was also examined (*1*, *2*, *5*−*8*), and the enzyme was identified as a heme-containing enzyme, similar to myoglobin and hemoglobin, since isocyanide was known to be a potential ligand of the iron in hemoproteins. Since these findings, the isocyanide complexes of a variety of ferrous P450s have been examined spectrophotometrically (*9*, *10*). The characteristic features of the optical spectra are the presence of two Soret bands for the ferrous enzymes; one of which is located at 430 and the other at 455 nm. The ratio of the two bands varies, depending on pH, ionic strength, size of the alkyl group of the isocyanide, the nature of the P450 species, and by single mutations inside the heme pocket (*6*, *11*−*13*). For example, the Soret band at 430 nm is predominant at pH 6 for the ethyl isocyanide complex of ferrous P450 from liver microsome of phenobarbital-treated rabbits, but the band at 455 nm is also present and its

† This work was supported in part by grants from the Structural Biology and the MR Science Programs in RIKEN (to Y.S.), by grant from the Special Postdoctoral Researcher's Program in RIKEN (to E.O.), and by a grant-in-aid for Scientific Research on Priority Areas (Molecular Metallics) from the Ministry of Education, Science, Culture, and Sports of Japan (to H.H. and Y.S.).

* To whom correspondence should be addressed. Phone: +81-791-58-2817. Fax: +81-791-58-2818. E-mail: yshiro@mailman.riken.go.jp.

‡ Himeji Institute of Technology.

§ Osaka University.

[1] Abbreviations: P450, cytochrome P450; P450nor, P450 from denitrifying fungus *Fusarium oxysporum*; P450cam, *d*-camphor hydroxylase of *Pseudomonas putida*; Thr243Val and Ser286Val, the P450nor mutants, in which Thr243 and Ser286 were replaced with valine, respectively; Mb, myoglobin.

10.1021/bi002225s CCC: $20.00 
Published on Web 02/08/2001

Table 1: Crystal Parameters, Data Collection, and Structure Refinement

| data set | P450nor($Fe^{2+}$) | P450nor($Fe^{3+}$) | P450cam($Fe^{2+}$) | P450cam($Fe^{3+}$) |
|---|---|---|---|---|
| temperature (K) | 100 | 100 | 100 | 293 |
| resolution range (Å) | 25.0−1.6 | 25.0−1.5 | 100.0−1.7 | 15.0−2.0 |
| reflections | | | | |
| measured/unique | 289017/47202 | 356663/57289 | 283735/40825 | 118057/27413 |
| completeness (%) | | | | |
| overall/outer shell | 91.9/81.0 | 92.4/65.3 | 91.7/67.6 | 95.1/79.8 |
| $R_{merge}$ (%)[a] | | | | |
| overall/outer shell | 5.5/37.1 | 5.6/27.8 | 5.9/35.8 | 3.3/5.4 |
| redundancy | 6.1 | 6.2 | 7.0 | 3.2 |
| **refinement statistics** | | | | |
| resolution range (Å) | 25.0−1.6 | 25.0−1.5 | 30.0−1.7 | 15.0−2.0 |
| $\sigma$ cutoff | 0.0 | 0.0 | 0.0 | 0.0 |
| reflections used | 47 158 | 57 245 | 40 718 | 27 340 |
| *R*-factor (%)[b] | 20.7 | 20.7 | 22.1 | 17.9 |
| free *R*-factor (%) | 25.8 | 24.1 | 27.1 | 22.5 |
| solvent | 285 | 303 | 179 | 162 |
| rms deviations from ideals | | | | |
| bond lengths (Å) | 0.008 | 0.007 | 0.011 | 0.006 |
| bond angles (deg) | 1.3 | 1.3 | 1.4 | 1.1 |
| Ramachandran plot | | | | |
| residues in most favorable regions (%) | 92.3 | 92.6 | 87.7 | 90.5 |
| residues in additional allowed regions (%) | 7.7 | 7.4 | 12.3 | 9.5 |
| residues in disallowed regions (%) | 0.0 | 0.0 | 0.0 | 0.0 |

[a] $R_{merge} = \sum|I_i - \langle I\rangle|/\sum I_i$, where $I_i$ is the intensity of an observation and $\langle I\rangle$ in the mean value for its unique reflection, and the summations are over all reflections. [b] *R*-facter $= \sum_h||F_o(h)| - |F_c(h)||/\sum_h F_o(h)$, where $F_o$ and $F_c$ are the observed and calculated structure factor amplitudes, respectively. free *R*-factor was calculated with 5% of the data excluded from refinement. Values in outer shell are for the highest resolution shell (the resolution of 1.5 Å was 1.58−1.50 Å; 1.6 A was 1.69−1.60 Å; 1.7 Å was 1.79−1.70 Å; 2.0 Å was 2.10−2.00 Å).

intensity increases when the pH is raised to 8 (*12*). At ambient pH, the ratio of the absorbances, $A_{430}/A_{455}$, is larger in this P450 than the other P450 from liver microsomes. In addition, it is also noteworthy that the double Soret bands in the optical absorption spectra of the ferrous isocyanide complexes have also been reported for other hemoproteins having a thiolate ($S^-$) as a fifth iron ligand for the case of nitric oxide synthase (*14*). Despite such extensive studies, the issue of the nature of the structural and/or electronic origin of the double Soret bands in these ferrous heme-enzymes remains unelucidated.

Most recently, Imai et al. reported that the isocyanide complex of P450 from denitrifying fungus *Fusarium oxysporum* (P450nor), gives a single Soret band at 427 nm, with a slight shoulder at 455 nm (*15*). This is in sharp contrast to another observation, which reported that a single Soret band was observed at 453 nm for the isocyanide complex of the *d*-camphor hydroxylase of *Pseudomonas putida* (P450cam) (*10*, *15*). Therefore, the finding by Imai et al. provides an opportunity to elucidate the 430 nm and the 450 nm species of the P450 isocyanide complexes in structural and/or electronic terms. Comparing crystal structures of both P450s, it was found that the basic structures, e.g., topology of the secondary structure, are identical. Therefore, the spectral difference should contribute to subtle but significant differences in structures of the heme moiety for their ferrous isocyanide complexes. To evaluate such structural differences, we spectrophotometrically and crystallographically compared the isocyanide coordination to the heme iron in P450nor and P450cam. This study provides new insight into the relationships between structure and properties of some metalloproteins.

## EXPERIMENTAL SECTION

*Materials.* Recombinant enzymes of P450nor and P450cam were used in this study. Their expression systems, purification procedure, and crystallization have been described elsewhere (*16*−*18*). The crystals of the *n*-butyl isocyanide complexes of the ferrous enzymes were prepared as follows. A crystal of the ferric form was placed in the mother liquid, which contained $Na_2S_2O_4$ under anaerobic conditions. A 2 $\mu$L aliquot of neat *n*-butyl isocyanide (Aldrich) was then added to the mother liquid, where the final concentration was about 50 mM. The color of the crystal immediately changed from reddish-brown ($Fe^{3+}$) to dark red ($Fe^{2+}$), and then to a pale red ($Fe^{2+}$-$CNC_4H_9$) after 5 min. The formation of the complexes was confirmed by measuring the optical spectra of the crystals (data not shown). The crystals of the ferric isocyanide complexes were prepared by soaking *n*-butyl isocyanide in the absence of $Na_2S_2O_4$.

*Methods. X-ray Crystallography.* Diffraction data for the isocyanide complexes of P450nor and P450cam were collected at BL44B2 (RIKEN BL2) in SPring-8, Harima, Japan (*19*). Data collection and processing and refinement were performed according to methods which have been reported previously (*17*, *20*). Statistics are given in Table 1. The structures of native P450nor (PDB ID, 1CL6) and P450cam (PDB ID, 2CPP), without the sixth ligand, were used as an initial model for structural refinement of the isocyanide complexes. After a first round of rigid-body, simulated annealing and *B*-factor refinements, a $|2F_o - F_c|$ map was calculated. A high electron density was found at the sixth iron position. Manual rebuilding of the isocyanide and water molecules was then carried out. Structural evaluations of the final models using PROCHECK indicated that more than

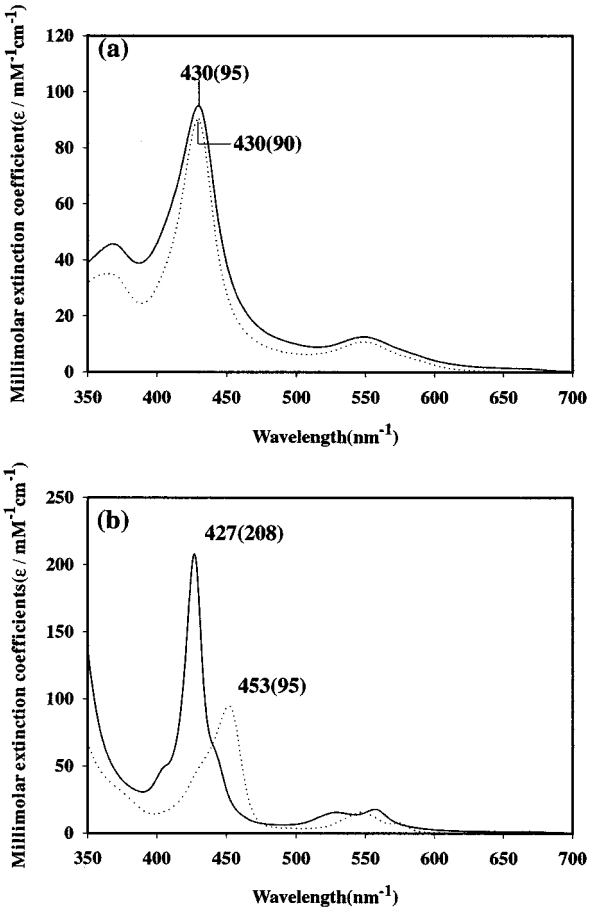


FIGURE 1: Optical absorption spectra of the isocyanide complexes of P450nor and P450cam in the (a) ferric and (b) ferrous states. Solid lines show the spectra of P450nor, while dotted lines show the spectra of P450cam. The samples were prepared in the 50 mM potassium phosphate buffer at pH 7.0. The values in parentheses indicate the molar coefficients of the Soret bands, which were determined by the pyridine hemochrome method.

93% of the residues are in the most favorable regions of the Ramachandram plot, and no residues are in disallowed regions. The coordinates of the isocyanide complexes of P450s have been deposited at RCSB Databank, in which their ID codes are 1GEI [P450nor($Fe^{2+}$-isocyanide)], 1GEJ [P450nor($Fe^{3+}$-isocyanide)], 1GEK [P450cam($Fe^{2+}$-isocyanide)] and 1GEM [P450cam($Fe^{3+}$-isocyanide)].

*Spectroscopies.* Infrared spectra were measured using SPECTRUM 2000, Perkin-Elmer Instrument. The sample concentration for the IR spectral measurement was about 2 mM. The $CaF_2$ cell was used for the water solution. EPR measurements were carried out at the X-band (9.23 GHz) microwave frequency using a Varian E-12 spectrometer, operated at a 100 kHz field modulation. An Oxford flow cryostat (ESR-900) was used for measurements at 15 K. The sample concentration for the EPR spectral measurement was about 1 mM.

## RESULTS

*Optical, EPR, and Infrared Spectra.* The optical absorption spectra of the *n*-butyl isocyanide complexes of P450s in the ferrous and ferric states are shown in Figure 1, panels a and b, respectively. In the case of the ferric isocyanide complexes (Figure 1a), the Soret absorption is located at 430 nm in the spectra of both P450cam and P450nor. On the other hand,

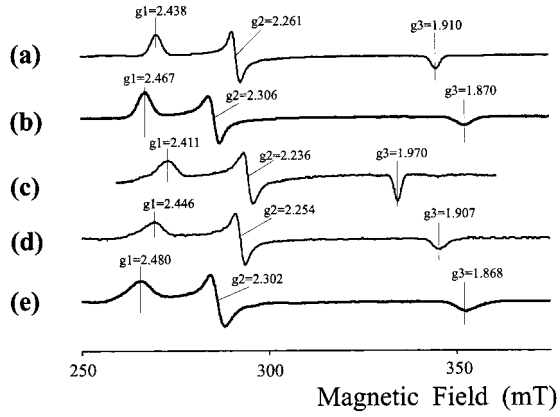


FIGURE 2: ESR spectra of (a) the ferric resting form of P450nor, (b) the ferric isocyanide complex of P450nor, (c) the *d*-camphor-bound form of ferric P450cam, (d) the *d*-camphor-free form of ferric P450cam, and (e) the ferric isocyanide complex of P450cam. These spectra were measured at 15 K. Sample concentrations were about 1 mM.

the single Soret band was located at 427 nm for the ferrous isocyanide complex of P450nor, while at 453 nm for that of P450cam (Figure 1b). These spectral features are identical to those reported previously (*15*). The pyridine hemochrome method (*21*) was used to determine the molar coefficient of the Soret band for each form, which are shown in parentheses in the spectra.

While the ferrous isocyanide complex is in a diamagnetic and therefore ESR-silent state, the ferric isocyanide complex is in a paramagnetic ($S = {}^1/_2$) state, thus giving EPR signals (*9*, *10*). Figure 2 shows the EPR spectra of the ferric isocyanide complexes of P450nor and P450cam, along with those of the ferric resting enzymes. As was the case for the ferric resting P450s, the isocyanide complexes gave EPR spectra characteristic for the heme iron in the ferric low spin, in which the signals with *g*-values, $g_1 = 2.47 \approx 2.48$, $g_2 = 2.30$, and $g_3 = 1.87$, are observed. This spectral feature was the same for the isocyanide complexes of the two enzymes. In addition, the spectra of the isocyanide complexes of P450cam, which were prepared from the camphor-bound and -free forms, were indistinguishable. The *g*-values are comparable to those ($g_1 = 2.32-2.3$, $g_2 = 2.24-2.32$, $g_3 = 1.94-1.86$) of the model compounds, which contain the mixed axial ligands of isocyanide and thiolate anion (*22*).

Most recently, Walker and co-workers (*23*) reported a unique EPR spectrum for the ferric bis-isocyanide complex of the iron-porphyrin, {(porphyrin)Fe[CN(*t*-$C_4H_9)_3]_2$}$ClO_4$, in which signals with $g = 2.20$ and 1.94 are observed. In combination with its NMR, IR, and Mossbauer spectral data, this spectral uniqueness was explained in terms of the characteristic electronic configuration of the iron in the complex, $(dxz, dyz)^4(dxy)^1$, resulting from the axial coordination of two isocyanide ligands. In contrast, the electronic configurationes of P450s is in a normal ferric low spin state, $(dxy)^2(dxz, dyz)^3$. The mixed-coordination of the isocyanide and the thiolate from Cys has no serious effect on the energy level of the iron dxy orbital, at least for the heme iron in the ferric low spin state.

To characterize the electronic structure of the heme in more detail, their IR spectra were measured. Figure 3(A) shows the region of the C−N stretching frequency of the iron-bound isocyanide in the IR spectra of P450nor and

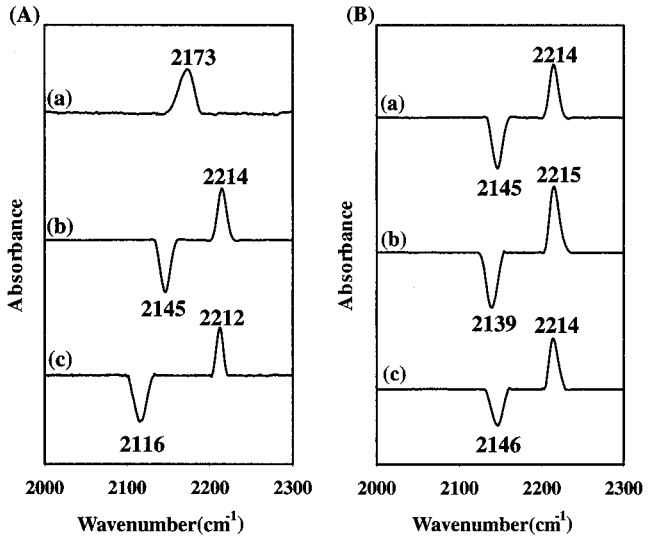


FIGURE 3: (A) C−N stretching region in the IR spectra of (a) the free isocyanide, (b) isocyanide bound to the heme iron of P450nor and (c) P450cam. (B) C−N stretching region in the IR spectra of (a) WT, (b) Thr243Val, and (c) Ser286Val for the isocyanide complexes of P450nor. All spectra are shown in the form of difference spectra between the ferric and the ferrous complexes.

P450cam. For comparison, the C−N stretching band of the free isocyanide (2170 $cm^{-1}$) is also shown in this figure. In the ferric form, the iron-bound isocyanide gave a C−N stretching frequency at 2213 $cm^{-1}$ for both enzymes. On coordination to the ferric iron, the C−N stretching is shifted to 43 $cm^{-1}$ in a higher frequency region. On the other hand, the C−N stretching bands for the ferrous complexes are located in the lower frequency region from the free isocyanide. These were observed at 2145 $cm^{-1}$ for P450nor, while at 2116 $cm^{-1}$ for P450cam. The observations of the IR spectra are consistent with the optical spectra; the electronic structures of the heme moiety are indistinguishable in the ferric isocyanide complexes, while, for the ferrous isocyanide complexes of P450nor and P450cam, significant differences are observed.

The IR spectra of the isocyanide complexes of the P450nor mutants, in which Ser286 or Thr243 was replaced with valine (Val) were also measured. This is mainly because the location of water molecules in the heme pocket are dramatically changed for these mutation, and, as a consequence, both mutants exhibit a very low enzymatic activity, compared with the wild-type (WT) enzyme (*17*, *20*, *24*). As illustrated in Figure 3B, for both mutants (Thr243Val and Ser286Val) in the ferric state, the C−N stretching frequencies of the iron-bound isocyanide are located at the same position (2214−5 $cm^{-1}$) as that of the WT enzyme. In contrast, the bands are observed at 2139 and 2146 $cm^{-1}$ for the ferrous Thr243Val (Figure 3B, spectrum b) and Ser286Val (Figure 3B, spectrum c) mutants, respectively. The band position is lower by 6 $cm^{-1}$ for Thr23Val, while it is at the same position for Ser286Val, compared with that for the WT P450nor (Figure 3B, spectrum a). The mutation effect will be discussed later in relation to the electronic structure of the isocyanide complex of P450nor.

*Crystal Structures of Isocyanide Complexes.* To understand similarities and/or differences in the coordination of the isocyanide, the crystal structures of the *n*-butyl isocyanide complexes of P450nor and P450cam in the ferric and the ferrous states are determined at cryogenic temperature. As shown in the side-view of the crystal structures (Figure 4, panels a and b), the *n*-butyl isocyanide coordinates to the ferrous iron in a slightly bent and tilt fashion, and the *n*-butyl chain is bent by about 90° at its Cα position. The coordination geometry, i.e., bond angles and bond lengths, are compiled in Table 2 and are compared for the P450nor and P450cam. In the comparison, the most remarkable difference is the bond angle, ∠Fe−C−N, 175° for P450nor, and 159° for P450cam. The coordination structures [d(Fe−C) and ∠Fe−C−N] of the isocyanide for each P450 were unchanged when the heme iron was oxidized from the ferrous to the ferric states, as shown in Figure 4, panels c and d, and Table 2. The bond angles can be compared with those in Mb and model systems. Olson et al. (*25*) found that the Fe−C−N angle is 106° in the crystal structures of the ethyl isocyanide complex of myoglobin (Mb). The highly bent coordination of the isocyanide in Mb is possibly due to a steric effect in the distal heme pocket. On the other hand, in the model system, {Fe(TPP)[CNC$(CH_3)_3]_2$}, the Fe−C−N angle is 168−9° (*23*). The slight deviation from the linear Fe−C−N was explained in terms of the crystal packing effects.

Table 2: Heme Coordination Geometry

| compd | proximal (Cys, His)−Fe distance (Å) | Fe−C (ligand) distance (Å) | Fe−C−N (ligand) angle (deg) |
|---|---|---|---|
| P450nor($Fe^{2+}$) | 2.36 | 1.85 | 175 |
| P450nor($Fe^{3+}$) | 2.33 | 1.86 | 171 |
| P450cam($Fe^{2+}$) | 2.30 | 1.86 | 159 |
| P450cam($Fe^{3+}$) | 2.24 | 1.82 | 149 |
| Myoglobin[a] | 2.28 | 2.13 | 143 |

[a] Protein Data Bank deposit code: 104M. Ligand was *n*-butyl isocyanide.

In Figure 5, the structures of the heme moiety are compared for the top view. The alkyl side chain of the iron-bound isocyanide is extended in the direction of the γ-meso position in the case of P450nor, while in the direction of the 7-propionate in P450cam, possibly in order to avoid steric congestion. In the case of P450cam (Figure 5b), the alkyl group of the isocyanide extends to the substrate binding site, and expels *d*-camphor, even though this complex was prepared in the presence of *d*-camphor (*26*, *27*). This observation is consistent with the EPR results mentioned above. This provides an explanation for why the $K_d$ value of the isocyanide from P450cam is varied depending on the concentration of *d*-camphor (*10*). In addition, the side chain of Val247 sterically pushes the Cα position of the iron-bound isocyanide (Figure 5b), resulting in the bent Fe−C−N bond.

The heme pocket of P450nor is intrinsically opened. In the close proximity of the iron-bound isocyanide in P450nor (Figure 5a), some hydrophilic side chains of amino acids, e.g., the OH groups of Ser286 and Thr243, as well as several water molecules are present, creating a hydrophilic environment. For example, the distances from the N atom of the iron-bound isocyanide are 4.40 Å to the Ser286 OH group, 4.22 Å to the Thr243 OH group and 3.03 Å to the main chain carbonyl O atom of Ala239. The water molecule bridging between the Ala239 O atom and the Thr243 OH group is located at a distance of 4.39 Å from the isocyanide N atom. Several water molecules are present over the iron-bound isocyanide in P450nor. These features are in sharp

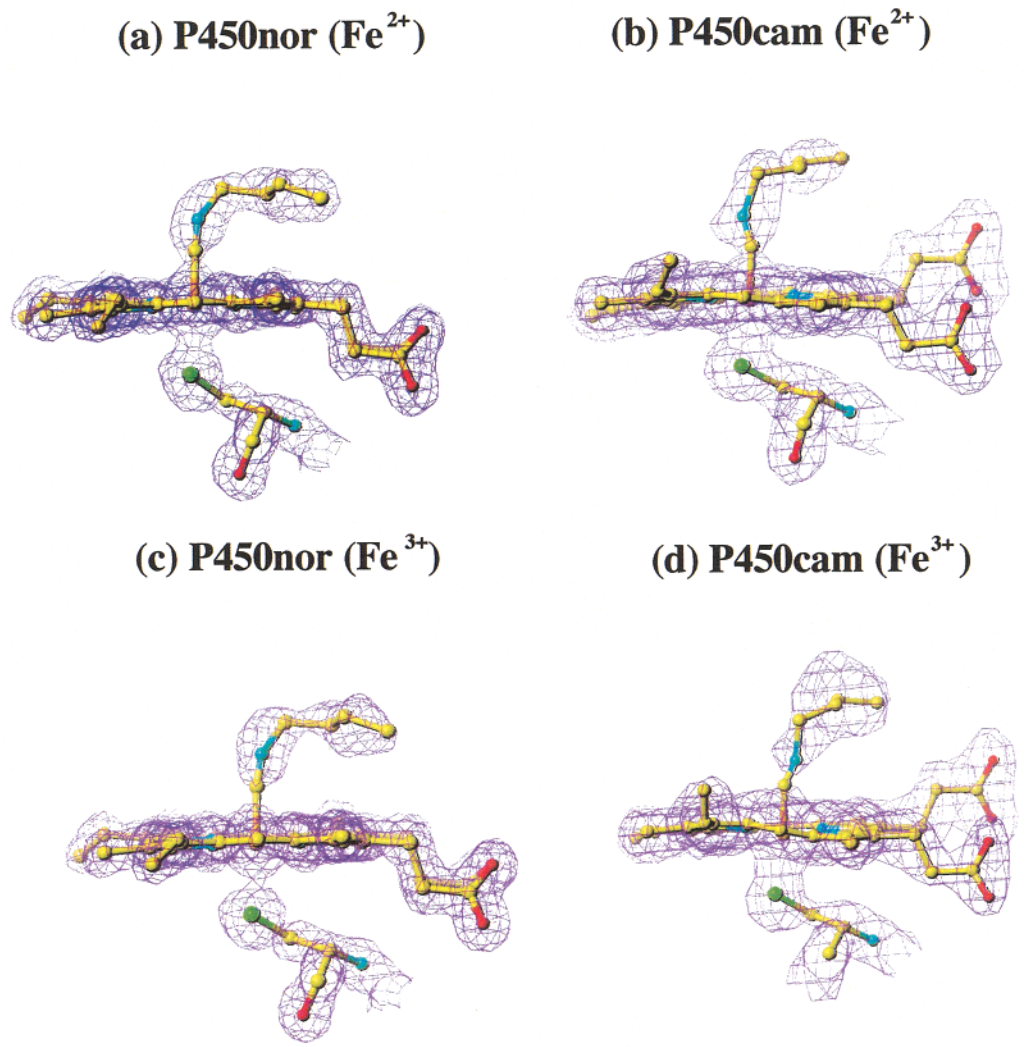


FIGURE 4: Side view of the heme moiety of the isocyanide complexes of (a) P450nor($Fe^{2+}$), (b) P450cam($Fe^{2+}$), (c) P450nor($Fe^{3+}$), and (d) P450cam($Fe^{3+}$). Electron density maps are fitted with the model structures, in which carbon atoms are represented in yellow, nitrogen atoms in blue, oxygen atoms in red, and sulfur atom in green.

contrast to the hydrophobic environment in the distal heme pocket which surrounds the iron-bound isocyanide in P450cam, as is illustrated in Figure 5b, in which the polar groups are located more than 5 Å from the isocyanide N atom and no water molecules are present in the close proximity of the iron-bound isocyanide.

The structures in the Cys-ligand loop at the fifth iron site are shown in Figure 6. The structure in this region is highly conserved in P450s, the crystal structures of which are available, and possibly in all P450s (*26*−*32*). For both P450nor and P450cam in the ferrous state, the coordination of the isocyanide ligand at the sixth position has no effect on the Cys-ligand loop structure. As shown in Table 2, the Fe−S bond distance is also unchanged on oxidation of the heme iron, within the accuracy of the X-ray crystallography.

## DISCUSSION

*Coordination Structure of Fe*−*CN(n-C*$_4$*H*$_9$*) in Ferric and Ferrous Cytochrome P450s.* The isocyanides are the only class of stable organic compounds which contain divalent carbon. Two possible representations for the isocyanide structure are described in Scheme 1 (33). R indicates an alkyl group, n-C4H9 in the present study. When the isocyanide

Scheme 1


(A) (B)

Scheme 2

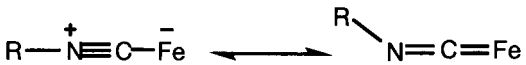


(C) (D)

coordinates to a transition metal, Fe in the case of hemoproteins, two resonance forms are possible (Scheme 2). The respective contribution of the two states is related to the oxidation state of the iron, the nature of the R group, the steric and chemical environments of the iron-coordinated isocyanide, and related factors.

In the IR spectra of the *n*-butyl isocyanide complexes of *ferric* P450s (Figure 3), the C−N stretching frequency of the iron-bound isocyanide was located at a higher frequency than that of the free isocyanide. The C−N bond is strengthened by coordination to the *ferric* iron of P450s, suggesting that the isocyanide ligand acts as a $\sigma$-donor to the iron rather than a $\pi$-acceptor. In other words, the back-donation from

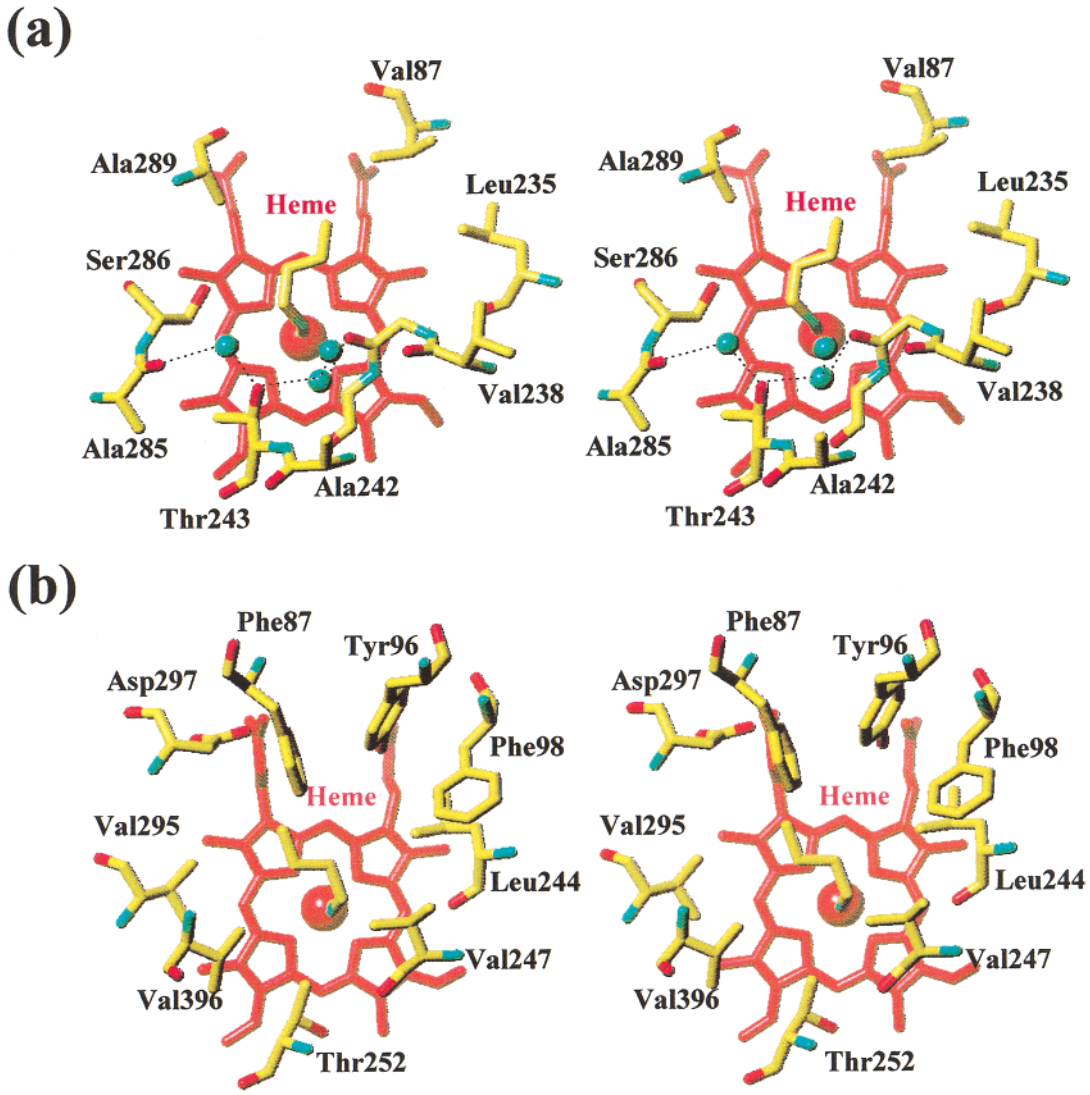


FIGURE 5: (Stereoview) Top view of the heme moiety of the isocyaniode complexes of (a) P450nor($Fe^{2+}$) and (b) P450cam($Fe^{2+}$). The amino acid side chains located within 10 Å above the heme plane (orange) are presented. Colors of the atoms are the same as those in Figure 4. Blue balls in panel a indicate the water molecules, and dotted line shows the hydrogen bond interaction.

the iron *d*-orbital to the ligand $\pi^*$-orbital is negligible or nonexistent. Therefore, the state of C is predominant in the resonance structure of the isocyanide complexes of *ferric* P450s. On the other hand, the lower-field shift of the C−N stretching frequency on coordination of isocyanide to the *ferrous* P450s suggests that the C−N bond is weakened, and that the isocyanide ligand acts as a $\pi$-acceptor. The back-donation to the axial ligand is facilitated, and consequently state D is predominant in the resonance structure (Scheme 2) of the *ferrous* isocyanide complexes.

The C−N stretching frequencies of the isocyanides in P450s were compared with those of the model systems (*34*−*36*). In the model systems, the C−N stretching shifts by 1−6 $cm^{-1}$ to a lower frequency on coordination to the *ferrous* iron, while that in the *ferric*-porphyrin model is located at a 70−95 $cm^{-1}$ higher frequency from that of the free isocyanide. This finding indicates that the isocyanide in the model systems acts as a good $\sigma$-donor but a poor $\pi$-acceptor, in sharp contrast to the P450 systems. The difference in the effect of coordination to the iron on the C−N stretching can be interpreted in terms of the trans effect, i.e., the effect of the fifth axial ligand of the Cys thiolate. The thiolate anion at the trans position would be expected to enhance the back-donation from the *ferrous* iron to the isocyanide, while retarding the $\sigma$-donation from the isocyanide to the *ferric* iron.

*Origin of 430 nm and 455 nm Species of Isocyanide Complexes of Ferrous Cytochrome P450nor and P450cam.* Several explanations have been proposed in order to explain the characteristic features in the optical absorption spectra of the isocyanide complexes of P450s: double Soret bands at 450 and 430 nm are present in the *ferrous* form, while a single Soret band at 430 nm is observed for the *ferric* form. For example, the Cys thiolate could be displaced or at least the Fe−S bond elongated, corresponding to the 430 nm species, which is the so-called cytochrome P420 (*33*). However, this explanation can be ruled out completely by the present crystallographic study. The thiolate ligand of Cys is present at the fifth position of the heme iron of both P450s in any state, and the Fe−S bond length and the structure at the Cys ligand loop is not largely altered as the result of the complex formation with isocyanide.

On the basis of the present IR spectral results, it is likely that the 430 nm species (i.e., the ferrous isocyanide complex of P450nor) gives a C−N stretching frequency around 2145 $cm^{-1}$, while the 450 nm species (i.e., the ferrous isocyanide

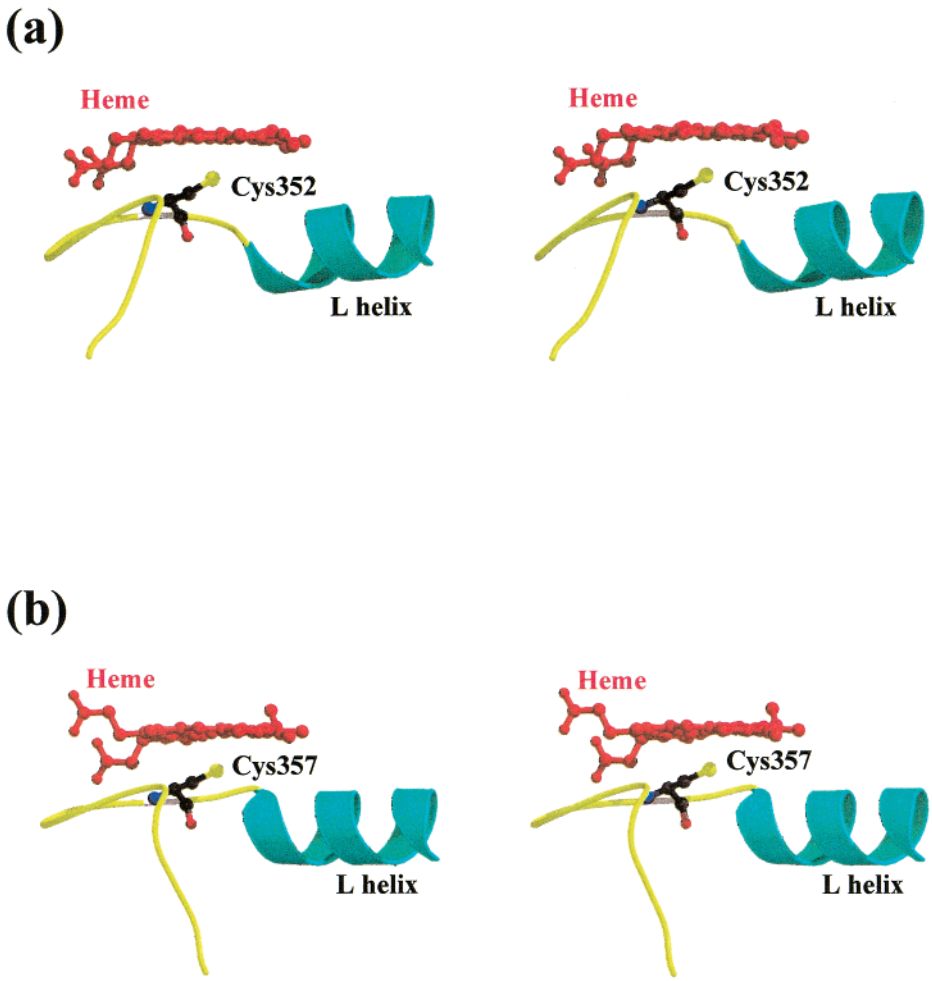


FIGURE 6: (Stereoview) Side view of the structure at the Cys-ligand loop (yellow) in the isocyanide complexes of (a) P450nor($Fe^{2+}$), and (b) P450cam($Fe^{2+}$). Sulfur atom coordinating to the heme iron as a fifth ligand is representative in yellow ball.

complex of P450cam) shows this at 2116 $cm^{-1}$. These spectral differences are possibly due to differences in the relative contribution of each state, C or D in Scheme 2, to the resonance form of the iron-isocyanide complex. As discussed in the previous section, this contribution is dependent on the degree of the back-bonding form of the iron atom. The relative contribution of state D in the resonance form would be increased when the back-donation from the iron to the ligand is increased. Therefore, the low-frequency shift of the C−N stretching frequency of the ferrous isocyanide complex of P450cam, compared to that of P450nor, can be explained in terms of increased back-donation. In contrast to the *ferrous* complexes, the contribution of state C to the resonance form is predominant in the *ferric* isocyanide complexes, as discussed in the preceding section.

The contribution of each state to the resonance structure would be expected to be modulated by structures around the heme-ligand moiety, the characteristics of which should be different between the isocyanide complexes of P450nor and P450cam. The present structural comparison shows that the prominent differences in the structures in the heme moiety between the two P450s are *the Fe−C−N coordination angle* and *the polarity around the isocyanide*.

*Steric Effect.* In state D, the isocyanide coordination has both $\sigma$ and $\pi$ bonding characteristics. In such coordination, p$\pi$(ligand) − d$\pi$(iron) interactions might be influenced by the Fe−C bond geometry, because of the asymmetry of the $\pi$-orbitals. In the case of the Fe−CO complexes of hemoproteins, the relationship of the distortion of the Fe−C bond to back-donation has been discussed previously (*37*, *38*); back-donation is increased when the Fe−CO bond is tilted or bent, as the result of increased overlap between the iron d- and the ligand $\pi$*-orbitals. According to the proposal on the Fe−CO complexes, it is likely that the tilted or bent Fe-isocyanide bond in P450cam facilitates back-donation, while the linear Fe-isocyanide bond in P450nor does not. Consequently, state D is more stabilized in the *ferrous* complexes of P450cam than of P450nor.

In contrast to state D, the Fe−CN bond in state C has symmetric $\sigma$ bonding characteristics. Therefore, the coordination geometry of the isocyanide would have no effect on the back-donation. Since state C is predominant in the *ferric* isocyanide complexes of P450s, the Fe-isocyanide bond in the ferric complexes is not influenced by this tilt or bent coordination. This provides an explanation for why the C−N stretching frequency is similar in the *ferric* isocyanide complexes of P450s.

*Polarity Effect.* The crystallographic results revealed that the vicinity of the iron-bound isocyanide is quite polar, in the case of P450nor, while apolar in P450cam. The polarity in the heme pocket should also influence the resonance forms shown in Scheme 2, because state C is polarized, while D is nonpolar. Here, we refer to a correlation between the polarity

Scheme 3

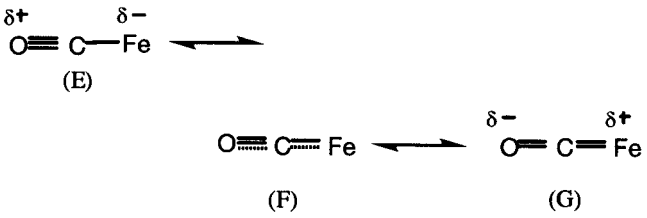


in the heme pocket and the CO coordination to the heme iron, which has been comprehensively discussed for Mb (*39*, *40*).

In this Scheme 3, the magnitude of the back-donation is in the order of G > F > E, and eventually, the CO stretching frequency is located from low to high frequencies in the order of G < F < E. The relative contribution of each state is determined by the polarity surrounding the iron-bound CO. Positive electrostatic potentials near the O atom increase the contribution of state G, while partially negative charge has opposite effect and increase the contribution of state E.

The knowledge on the iron-bound CO could be applicable to the resonance forms of C and D in the iron-bound isocyanide (Scheme 2). In the *ferrous* isocyanide complexes, state D is predominant, but state C also contributes to the resonance form, to some extent. A partially and/or fully negative charge in the distal pocket would be expected to promote the contribution of C in the resonance form. Indeed, O($\delta$-)H groups and $H_2O$($\delta$-) molecules are present in the heme pocket of P450nor (see Figure 5a), thus facilitating the contribution of state C. On the other hand, the apolar heme pocket of P450cam exerts no effect on the resonance form.

Since the polarized state, C, of the iron-isocyanide moiety is primarily stabilized in the *ferric* complex of P450s, the polarity in the heme pocket does not affect the electronic state in the resonance form. Consequently, no difference was observed for the C−N stretching frequencies in the IR spectra between P450cam and P450nor. Our proposal could be verified by the mutation effect on the IR data of the isocyanide complexes in P450nor. The C−N stretching frequency was unaltered in the ferric form by the Thr243 and Ser286 mutations, while, in the ferrous form, it was shifted to the lower frequency (an increment in the contribution of state C) on removal of the OH group from the 243 position. It is not presently clear why the removal of the OH group at the 286 position has such a small effect on the C−N stretching frequency in P450nor. One possible reason is that the different orientation of the OH groups relative to the bound isocyanide, between Ser286 and Thr243 (Figure 5a), might exert different effects. The dipole−dipole interaction is maximum when the vectors are parallel with respect to each other, while it is zero when the vectors interact with $3\cos^2\theta = 1$, where $\theta$ is an angle between two dipoles. Therefore, the interaction between the dipole vector made by the Ser286 OH group and that of the iron-bound isocyanide might be small.

The present crystallographic and spectroscopic studies show that the double Soret bands in the optical absorption spectra of the ferrous isocyanide complexes of P450 are caused by differences in the characteristics of the Fe-isocyanide bond, suggesting that either steric effects, polarity in the heme pocket or a combination of both significantly affect the nature of the iron-isocyanide bond. In the case of isocyanide complexes of general P450s, the protein conformations giving the electronic state of the P450nor type (the 430 nm species) and of the P450cam type (the 450 nm species), which are so-called conformational isomers (conformers) with each other, are in equilibrium depending on the pH, ionic strength, single mutations. It seems likely that protonation or deprotonation directly and/or indirectly modulates the steric factors and/or the polarity of the heme distal pocket, eventually changing the equilibrium between the two conformers.

Last, we wish to mention the effects of the steric and chemical environments on the C−O stretching frequency of the iron-bound CO between P450nor and P450cam. Since the CO molecule is a good $\pi$-acceptor, state G in Scheme 3 is highly stabilized in the case of P450s by the trans effect from the fifth $S^-$ ligand. In this situation, neither the polarity nor steric effects no longer exert any influence on the Fe−CO electronic structure, eventually giving rise to the C−O stretching at 1942 $cm^{-1}$ for both enzymes (*41*). Therefore, the unique properties of the iron-bound isocyanide, which were examined in this study, are predicted to be due to the poor $\pi$-acceptor characteristics (*42*).

## ACKNOWLEDGMENT

We thank Dr. Shin-ichi Adachi for his assistance in the X-ray diffraction measurements at BL44B2 (RIKEN BL2) of SPring-8, and Prof. Yoshiro Imai for his encouragement.

## REFERENCES

1. Omura, T., and Sato, R. (1962) *J. Biol. Chem. 237*, 1375−1376.
2. Omura, T., and Sato, R. (1964) *J. Biol. Chem. 239*, 2370−2385.
3. Ortiz de Montellano, P. R., Ed. (1995) *Cytochrome P450. Structure, mechanism, and biochemistry*, 2nd ed., Plenum Press, New York.
4. Nelson, D. R., Koymans, L., Kamataki, T., Stegeman, J. J., Feyereisen, R., Waxman, D. J., Waterman, M. R., Gotoh, O., Coon, M. J., Estabrook, R. W., Gunsalus, I. C., and Nebert, D. W. (1996) *Pahrmacogenetics 6*, 1−42.
5. Nishibayashi, H., Sato, R., and Omura, T. (1966) *Biochim. Biophys. Acta 118*, 651−654.
6. Imai, Y., and Sato, R. (1966) *Biochem. Biophys. Res. Commun. 23*, 5−11.
7. Imai, Y., and Sato, R. (1967) *J. Biochem. 62*, 464−473.
8. Imai, Y., and Sato, R. (1968) *J. Biochem. 63*, 370−379.
9. Ichikawa, Y., and Yamano, T. (1968) *Biochim. Biophys. Acta 153*, 753−765.
10. Griffin, B., and Peterson, J. A. (1971) *Arch. Biochem. Biophys. 145*, 20−229.
11. Imai, Y., and Sato, R. (1968) *J. Biochem. 63*, 270−273.
12. Hashimoto-Yutsudo, C., Imai, Y., and Sato, R. (1980) *J. Biochem. 88*, 505−516.
13. Imai, Y., and Nakamura, M. (1989) *Biochem. Biophys. Res. Commun. 158*, 717−722.
14. Yoneyama, H., Hori, H., and Ichikawa, Y. (1997) *Biochim. Biophys. Acta 1335*, 253−264.
15. Imai, Y., Okamoto, N., Nakahara, K., and Shoun, H. (1997) *Biochim. Biophys. Acta 1337*, 66−74.
16. Park, S.-Y., Shimizu, H. Adachi, S., Shiro, Y., Iizuka, T., Nakagawa, A., Tanaka, I., Shoun, H., and Hori, H. (1997) *FEBS Lett. 412*, 346−350.
17. Park, S.-Y., Shimizu, H., Adachi, S., Nakagawa, A., Tanaka, I., Nakahara, K., Shoun, H., Nakamura, H., Iizuka, T., and Shiro, Y. (1997) *Nat. Struct. Biol. 4*, 827−832.

18. Imai, M., Shimada, H., Watanabe, Y., Matsushima-Hibiya, Y., Makino, R., Koga, H., Horiuchi, T., and Ishimura, Y. (1989) *Proc. Natl. Acad. Sci. U.S.A. 86*, 7823−7827.
19. Adachi, S., Oguchi, T., and Ueki, T. (1996) *Spring-8 Annual Report*, 239−240.
20. Shimizu, H., Park, S.-Y., Lee, D.-S., and Shiro, Y. (2000) *J. Inorg. Biochem. 81*, 191−205.
21. Antonini, E., and Brunori, M., Eds. (1971) *Hemoglobin and Myoglobin in Their Reactions with Ligands*, pp 10−11, North-Holland Publishing Company, Amsterdam.
22. Ruf, H. H., Wende, P., and Ullrich, V. (1979) *J. Inorg. Biochem. 11*, 189−204.
23. Walker, A. F., Nasri, H., Turowska-Tyrk, I., Mohanrao, K., Watson, C. T., Shokhirev, N. V., Debrunner, P. G., and Scheidt, W. R. (1996) *J. Am. Chem. Soc. 118*, 12109−12118.
24. Okamoto, N., Imai, Y., Shoun, H., and Shiro, Y. (1998) *Biochemistry 37*, 8839−8847.
25. Johnson, K. A., Olson, J. S., and Phillips, Jr., G. N. (1989) *J. Mol. Biol. 207*, 459−463.
26. Poulos, T. L., Finzel, B. C., and Howard, A. J. (1987) *J. Mol. Biol. 195*, 687−700.
27. Poulos, T. L., Finzel, B. C., and Howard, A. J. (1986) *Biochemistry 25*, 5314−5322.
28. Cupp-Vickery, J. R., and Poulos, T. L. (1995) *Nat. Struct. Biol. 2*, 144−153.
29. Hasemann, C. A., Ravichandran, K. G., Peterson, J. A., and Deisenhofer, J. (1994) *J. Mol. Biol. 236*, 1169−1185.
30. Ravichandran, K. G., Boddupalli, S. S., Hasemann, C. A., Peterson, J. A., and Deisenhofer, J. (1993) *Science 261*, 731−736.
31. Peterson, J. A., and Graham-Lorence, S. E. (1995) in *Cytochrome P450. Structure, mechanism, and biochemistry* (Ortiz de Montellano, P. R., Ed.) 2nd ed., pp 151−180, Plenum Press, New York.
32. Poulos, T. L., Cupp-Vickery, J., and Li, H. (1995) in *Cytochrome P450. Structure, mechanism, and biochemistry* (Ortiz de Montellano, P. R., Ed.) 2nd ed., pp 125−150, Plenum Press, New York.
33. Simonneaux, G., and Bondon, A. (2000) in *The Porphyrin Handbook* (Kadish, K. M., Smith, K. M., and Guilard, R. Eds.) Vol. 5, pp 299−322, Academic Press, New York.
34. Le Plouzennec, M., Bondon, A., Sodano, P., and Simonneaux, G. (1986) *Inorg. Chem. 25*, 1254−1257.
35. Jameson, G. B., and Ibers, J. A. (1979) *Inorg. Chem. 18*, 1200−1208.
36. Simonneaux, G., Hindre, F., and Le Plouzennec, M. (1989) *Inorg. Chem. 28*, 823−825.
37. Kuriyan, J., Wilz, S., Karplus, M., and Petsko, G. A. (1986) *J. Mol. Biol. 192*, 133−154.
38. Makinen, M. W., Houtchens, R. A., and Caughey, W. S. (1979) *Proc. Natl. Acad. Sci. U.S.A. 76*, 6042−6046.
39. Springer, B. A., Sligar, S. G., Olson, J. S., and Phillips, G. N., Jr. (1994) *Chem. Rev. 94*, 699−714.
40. Li, T., Quillin, M. L., Phillips, G. N., Jr., and Olson, J. S. (1994) *Biochemistry 33*, 1433−1446.
41. Shiro, Y., Kato, M., Iizuka, T., Nakahara, K., and Shoun, H. (1994) *Biochemistry 33*, 8673−8677.
42. Cotton, F. A., Wilkinson, G., Murillo, C. A., and Bochmann, M. (1999) *Advanced Inorganic Chemistry*, 6th ed., p 246, John Wiley & Sons, inc.

BI002225S